OPEN

Elevated Abundance, Size, and MicroRNA Content of Plasma Extracellular Vesicles in Viremic HIV-1+ Patients: Correlations With Known Markers of Disease Progression

Audrey Hubert, MSc, Caroline Subra, PhD,* Mohammad-Ali Jenabian, DVM, PhD,† Pierre-François Tremblay Labrecque, BSc,* Cécile Tremblay, MD,‡ Benoit Laffont, PhD,* Patrick Provost, PhD,* Jean-Pierre Routy, MD,§ and Caroline Gilbert, PhD**

Background: Because of factors only partly understood, the generalized elevated immune activation and inflammation characterizing HIV-1–infected patients are corrected incompletely with antiretroviral therapy (ART). Extracellular vesicles (EVs) including exosomes and microvesicles released by several cell types may contribute to immune activation and dysfunction. EV size, abundance, and content appear to differ according to infection phase, disease progression, and ART.

Methods: We examined whether the size of EVs and the abundance of exosomes in plasma are associated with cell and tissue activation as well as with viral production. Acetylcholinesterase-bearing (AChE+) exosomes in plasma were quantified using an AChE assay. EV size was analyzed using dynamic light scattering. Proteins and microRNAs present in EVs were detected by Western blot and real-time polymerase chain reaction, respectively.

Results: Exosomes were found more abundant in the plasma of ART-naive patients. EV size was larger in ART-naive than in ART-suppressed patients, elite controllers, or healthy control subjects. Both exosome abundance and EV sizes were inversely correlated with CD4/CD8 T-cell ratio and neutrophil, platelet, and CD4 T-cell counts and positively correlated with CD8 T-cell counts. A negative correlation was found between CD4 T-cell nadir and exosome abundance, but not EV size. Levels of miR-155 and miR-223 but not miR-92 were strongly correlated negatively with EV abundance and size in ART-naive patients.

Conclusions: Monitoring of circulating EVs and EV-borne microRNA is possible and may provide new insight into HIV-1 pathogenesis, disease progression, and the associated inflammatory state, as well as the efficacy of ART and the treatments intended to reduce immune activation.

Key Words: biomarker, CD4/CD8 T-cell ratio, DAP-3, exosomes, inflammation, HIV-1, microvesicles, microRNA, miR-155, miR-223

(*J Acquir Immune Defic Syndr* 2015;70:219–227)

INTRODUCTION

Several aspects of the immune response are deregulated rapidly and irreversibly during the acute phase of HIV-1 infection. By inhibiting HIV-1 viral replication, antiretroviral therapy (ART) improves immune function and effectively minimizes the risk of AIDS-related complications, albeit without restoring full health. HIV-infected patients under ART still present with elevated risks of cardiovascular, liver, kidney, and neurological disorders.[1] The severity of these non–AIDS-related complications is often proportional to the degree of immune activation and inflammation.[1] Elite controllers, who spontaneously control HIV-1 replication, are no exception and are also susceptible to immune activation and inflammation.[2] The factors underlying immune deregulation and elevated state of inflammation are not fully understood but include low persistent viral replication, fibrosis of lymphoid tissue, and translocation of microbial products from the gut, the latter leading to monocyte activation.[3] All of these factors contribute to enhancing T-cell apoptosis, although homeostatic factors help to maintain a stable pool of T cells.[4] In the context of

Received for publication December 14, 2014; accepted June 1, 2015.

From the *Centre de recherche du CHU de Québec and Faculty of Medicine, Département de microbiologie infectiologie et immunologie, Université Laval, Québec, Québec, Canada; †Département des Sciences Biologiques et Centre de recherche BioMed, Université du Québec à Montréal (UQAM), Montréal, Québec, Canada; ‡Centre de Recherche du Centre Hospitalier de l'Université de Montréal, Département de microbiologie infectiologie et immunologie, Montréal, Québec, Canada; and §Chronic Viral Illness Service and Research Institute, McGill University Health Centre, Montréal, Québec, Canada.

Supported through Grants MOP-188726 and MOP-267056 (HIV/AIDS Initiative) to C.G. and MOP-03230 to J.-P.R. and C.T. for cohort establishment and by the FRQ-S AIDS and Infectious Diseases Network. C.S. holds a CIHR Fellowship. C.T. is a FRQ-S Scholar and holder of the Pfizer/University of Montréal Chair on HIV Translational Research. B.L. is supported by a PhD Fellowship from the Canadian Blood Services. J.-P.R. holds the Louis Lowenstein Chair in Hematology and Oncology at McGill University. C.G. is a recipient of a New Investigator Award from the CIHR/HIV/AIDS Initiative.

The authors have no funding or conflicts of interest to disclose.

A.H., C.S., M.-A.J., B.L., and C.G. conceived and designed the experiments. A.H., C.S., and P.-F.T.L. performed the experiments. A.H., C.S., P.-F.T.L., M.-A.J., B.L., P.P., and C.G. analyzed the data. C.T., J.-P.R., P.P., and C.G. contributed clinical sample/reagents/materials/analysis tools. A.H., C.S., M.-A.J., J.-P.R., and C.G. wrote the article.

Correspondence to: Caroline Gilbert, PhD, Centre de recherche du CHU de Québec, T1-49, 2705 Boulevard Laurier, Québec, Québec G1V 4G2, Canada (e-mail: caroline.gilbert@crchul.ulaval.ca).

untreated infection and to a lesser degree with ART, infected CD4 T cells die by apoptosis.[5,6] An interesting recent study[7,8] suggests that while productively infected CD4 T cells die by caspase-3–dependent apoptosis, uninfected or abortively infected bystander CD4 T cells may die by pyroptosis, an inflammatory form of caspase-1–dependent cell death. This enhanced cell death promotes the release of microvesicles (MVs) and apoptotic bodies into the extracellular milieu.[9,10] These may contain certain HIV proteins such as Nef, which is associated with infectivity and disease progression.[11] The role of these vesicles as carriers of bioactive molecules in transmitting proinflammatory or anti-inflammatory signals to neighboring or target cells is known.[10,12]

Depending on their activation state, cells can produce different types of extracellular vesicles (EVs), most notably plasma membrane vesicles (MVs), exosomes, and apoptotic bodies.[10,13,14] Erythrocytes, leucocytes, and tumor cells are among the cell types that release EVs.[13,14] Exosomes are a type of EV originating in internal endocytic compartments called multivesicular bodies. They are released from viable cells into the extracellular milieu upon fusion of these bodies with the plasma membrane[13,14] and thus can be recovered from blood, urine, and saliva. The exosome surface and lumen harbor proteins and other macromolecules such as mRNA and microRNA that reflect their cell origin. In addition exosomes act as intercellular messengers that may modulate tolerance, antigen presentation, and inflammation.[13,14] MicroRNA is single-stranded noncoding RNA, 22 nucleotides in length, and capable of recognizing specific mRNA and inhibiting its translation into proteins, thereby influencing and altering numerous cellular functions.[15] These molecules may thus promote the development and function of hematopoietic stem cells[16] and regulate the immune system and inflammatory processes.[17] A microRNA known as miR-155 is involved in the innate and adaptive responses and regulates CD8 and Th17 cell differentiation.[18] Another microRNA of interest is miR-223, which is known for its role in infection, inflammation, and hematopoietic cell differentiation,[19,20] while miR-92 is associated with tumor cell proliferation.[21]

Exosomes circulating in biological fluids such as plasma may regulate multiple pathways in neighboring or distant cells through the delivery of genetic material. As the exosome content is altered by disease or treatment, they have been used as biomarkers in the monitoring of cancer[22] and viral infections including Epstein–Barr and hepatitis C.[23,24] Exosomes derived from dendritic cells (DCs) loaded with HIV-1 may regulate apoptosis of recipient cells, possibly due to death-associated protein 3 (DAP-3) and apoptotic protease-activating factor 1 (Apaf-1), 2 effector proteins involved in apoptosis,[25] and/or to Nef protein.[26] Exosomes have been shown to enhance trans HIV-1 infection in a paracrine manner,[25–30] whereas high levels of apoptotic MVs may induce DC dysfunction during acute HIV-1 infection[31] and facilitate infection of macrophages.[32] EVs and more precisely exosomes are now known to induce under certain pathological conditions dysfunctional innate and adaptive immune responses through their specific cargo.[10,13,14]

Studying the role of exosomes in the context of HIV-1 infection has proven to be a daunting challenge because the viral particles present biophysical characteristics very similar to those of exosomes, notably size, sedimentation rate on sucrose density gradient, and the presence of various molecules. Separation and characterization of exosomes in the presence of MV and HIV-1 require a specifically adapted technology. Using velocity-gradient centrifugation, acetylcholinesterase (AChE) activity measurement, and transmission electron microscopy, we and other groups have been successful at separating exosomes from virions, MVs, and apoptotic MV[25–28,30,33,34] and confirming that AChE+ vesicles are exosomes. To gain further insight into circulating exosomes and MVs in the context of HIV-1 infection, we analyzed the relative abundance of exosomes, the size distribution of heterogeneous populations of EV, and the presence of specific proteins and selected microRNA in plasma isolated from HIV-1–infected patients and investigated their association with various markers of immune status and disease progression.

MATERIALS AND METHODS

Studied Population

Forty-three HIV-1–infected patients participated: 17 ART-naive (having never received ART), 13 ART-treated with undetectable viral load (≤50 copies per milliliter of plasma), and 13 elite controllers (who spontaneously control viral replication in the absence of treatment). Sixteen healthy uninfected control subjects also participated. This study received approval from the Ethics Review Boards of the McGill University Health Centre, Montréal, Québec, Canada, and the Centre de recherche du CHU de Québec, Québec, Canada. All subjects were volunteers and provided written informed consent to participate in the study.

EV Purification

ExoQuick was used to precipitate and concentrate all EVs from plasma, including virions. Briefly, 250 μL of plasma was incubated overnight with 63 μL of ExoQuick reagent (SBI via Cedarlane, Burlington, ON, Canada) and centrifuged for 30 minutes at 1,500*g*, and the pellet was washed and then resuspended in a final volume of 250 μL of filtered (0.22 μm) phosphate-buffered saline. An AChE activity assay was used to determine exosome abundance.[33]

Western Blot Characterization of Proteins

The EV pellet (20 μL) precipitated from pooled plasma (13 samples) from each group using ExoQuick was added to 20 μL of modified Laemmli 2× sample buffer and kept at 100°C for 7 minutes as described previously.[35] The samples were then subjected to sodium dodecyl sulfate–polyacrylamide gel electrophoresis and transferred to Immobilon polyvinylidene fluoride membrane (Millipore Corporation, Bedford, MA). Before incubation with primary antibodies and secondary antibody, the membrane was blocked with nonfat skim milk solution (powdered milk dissolved at a concentration of 5% in Tris buffer saline with 0.1% Tween 20). Immunoblotting was performed overnight at 4°C using antibody diluted in nonfat skim milk solution. Anti–ICAM-1 (G-5, diluted at 1/200), anti–tumor

susceptibility gene 101 (TSG-101) (4A10, diluted at 1/200), and anti–DAP-3 (10/DAP3, diluted at 1/200) were purchased from Santa Cruz Biotechnology Inc. (Santa Cruz, CA), Abcam Inc. (Toronto, ON, Canada), and BD Transduction Laboratories (Mississauga, ON, Canada), respectively. Membranes were then washed twice in Tris buffer saline with Tween 20, incubated for 30 minutes with horseradish peroxidase-conjugated secondary anti-mouse antibody (Jackson ImmunoResearch, Mississauga, ON, Canada) at a dilution of 1/10,000, and revealed using a Luminata Forte Western horseradish peroxidase substrate from Millipore Corporation.

EV Size Measurement

Dynamic light scattering (DLS) was used to measure particle size in heterogeneous MV populations. These were precipitated using ExoQuick and resuspended in filtered (0.22 μm) phosphate-buffered saline (diluted at 1:2) in 4% paraformaldehyde. Size was determined in triplicate from light diffusion due to particle Brownian motion measured at 4°C using a Zetasizer Nano S (Malvern Instruments, Ltd., Malvern, United Kingdom).

Electron Microscopy

Briefly, 20 μL of ExoQuick pellet was fixed with an equal volume of 2% paraformaldehyde and concentrated on a formvar-coated electron microscopy grid using an Airfuge ultracentrifuge (Beckman, Palo Alto, CA) at 120,000*g* (air pressure of 20 psig) for 15 minutes. The grids were dried on bibulous paper and stained for 1 minute with a drop of 1% of uranyl acetate solution. The concentration, shape, and overall appearance of the EVs were examined using a FEI Tecnai Spirit G2 transmission electron microscope equipped with an AMT CCD camera.

MicroRNA Quantification in EVs Isolated From Plasma

Plasma samples (250 μL) were treated with proteinase K (final concentration of 1.25 mg/mL) for 10 minutes at 37°C and then centrifuged at 17,000*g* for 30 minutes. EVs in the supernatant were purified using ExoQuick as described above. The resulting pellet was diluted in TRIzol LS (Ambion, Life Technologies, Carlsbad, CA) at a ratio of 3:1 and stored at −80°C. Total RNA was extracted and resuspended in 12 μL of DEPC water. Reverse transcription was performed according to the manufacturer's instructions on 10 μL of this suspension using a HiFlex miScript RT II Kit (Qiagen, Hilden, Germany). Mature miR-155 (#MS00031486), miR-223 (#MS00003871), and miR-92 (#MS00006594) were detected by quantitative polymerase chain reaction using miScript Primer Assay Kit and miScript SYBR Green PCR Kit (Qiagen). Amplification of mature microRNA as cDNA was performed in Rotor-Gene 3000 operated with software version 6.1 (Corbett Life Science, Concorde, Australia) using 40 cycles of 95°C for 15 seconds, 55°C for 30 seconds, and 70°C for 30 seconds. Reaction specificity was ascertained by performing the Melt procedure (58–99°C, 1°C per 5 seconds) at the end of the amplification protocol according to the manufacturer's instructions. MicroRNA level was expressed in terms of cycle threshold (Ct). Ct values above 40 were considered negative.

Statistical Analysis

Data are presented as mean ± SEM. Treatment mean values were compared using single-factor analysis of variance followed by Tukey multiple comparisons. Bartlett test was applied to analyze variance between groups. Correlation coefficients were calculated using Spearman rank correlation

TABLE 1. Clinical Characteristics of the Studied Population

		HIV-1–Positive Subjects		
	Healthy Subjects (n = 16)	ART-Naive (n = 17)	ART-Suppressed (n = 13)	Elite Controllers (n = 13)
Viral load, $\log_{10}$ copies/mL	NA	4.0 ± 1.07	<1.7	<1.7
Years of infection	NA	1.68 ± 1.20	8.08 ± 3.5*†	12.8 ± 3.46*†‡
CD4, cells/μL	863.9 ± 163.4	445.8 ± 257.6†§	579.5 ± 192.7§‖	647.6 ± 237.5§¶
CD8, cells/μL	384.1 ± 146.8	843.8 ± 366.7†§	808.8 ± 230.5†§	574.8 ± 238.3*¶
CD4/CD8 ratio	2.5 ± 0.83	0.62 ± 0.45†§	0.77 ± 0.33†§	1.29 ± 0.52*†§¶
Neutrophils, $\times10^9$/L	4.4 ± 2.26	2.6 ± 1.51§¶	3.0 ± 0.63	3.70 ± 1.73
Monocytes, $\times10^9$/L	0.59 ± 0.21	0.48 ± 0.24	0.41 ± 0.12	0.60 ± 0.24
Platelets, $\times10^9$/L	235.1 ± 51.11	199.5 ± 73.85	234.6 ± 63.18	277.1 ± 117.7
Age, yrs	43.6 ± 7.83	34.18 ± 9.20§¶	44.7 ± 9.01*¶	47.1 ± 6.67*‖
Gender (women), n (%)	2 (12.5)	2 (11.8)	3 (23.1)	5 (38.5)
Men, n (%)	14 (87.5)	15 (88.2)	10 (76.9)	8 (61.5)

All clinical parameters are reported as mean ± SD.
*P value vs. ART-naive subjects.
†$P < 0.001$ (ANOVA, Tukey post test).
‡P value vs. ART-suppressed subjects.
§P value vs. healthy subjects.
‖$P < 0.01$ (ANOVA, Tukey post test).
¶$P < 0.05$ (ANOVA, Tukey post test).
ANOVA, analysis of variance; NA, not applicable.

test. All statistical analyses were performed using GraphPad Prism 5 software; P values <0.05 were deemed statistically significant. Asterisks denote the degree of significance ($*P < 0.05$, $**P < 0.01$, $***P < 0.001$).

RESULTS

Characterization of EVs Found in Plasma From HIV-1–Infected Patients

We have shown previously that DCs, the first immune cell type to come into contact with viral particles during the earliest phase of mucosal HIV-1 infection, subsequently release AChE+ vesicles called exosomes in larger than normal quantities.[25] We therefore tested the hypothesis that EVs found in plasma are indicative of cellular activation and in vivo HIV-1 replication by comparing healthy individuals and HIV-1–infected patients. Patient characteristics are summarized in Table 1. Figure 1A shows that the abundance of AChE+ exosomes in plasma is greater in ART-naive HIV-1–infected patients than in uninfected control subjects and elite controller patients ($P < 0.001$ for all comparisons). The similarity between levels in elite controllers and uninfected control subjects was striking (expressed as OD 450 nm/min: ART-naive: 52.31 ± 5.72; healthy subjects: 24.77 ± 3.93; ART-suppressed: 40.32 ± 5.91; elite controllers: 21.17 ± 4.25; $P < 0.001$ for comparisons between ART-naive and healthy subjects or elite controllers).

The plasma fraction precipitated using ExoQuick includes exosomes and plasma membrane–associated apoptotic MV as well as any viral particles present. In addition, analysis of EV size based on DLS (Figs. 1B, C) showed that EVs found in the plasma of ART-naive patients were of larger and more broadly distributed diameter than those from any other group of subjects (in nanometer: healthy subjects:

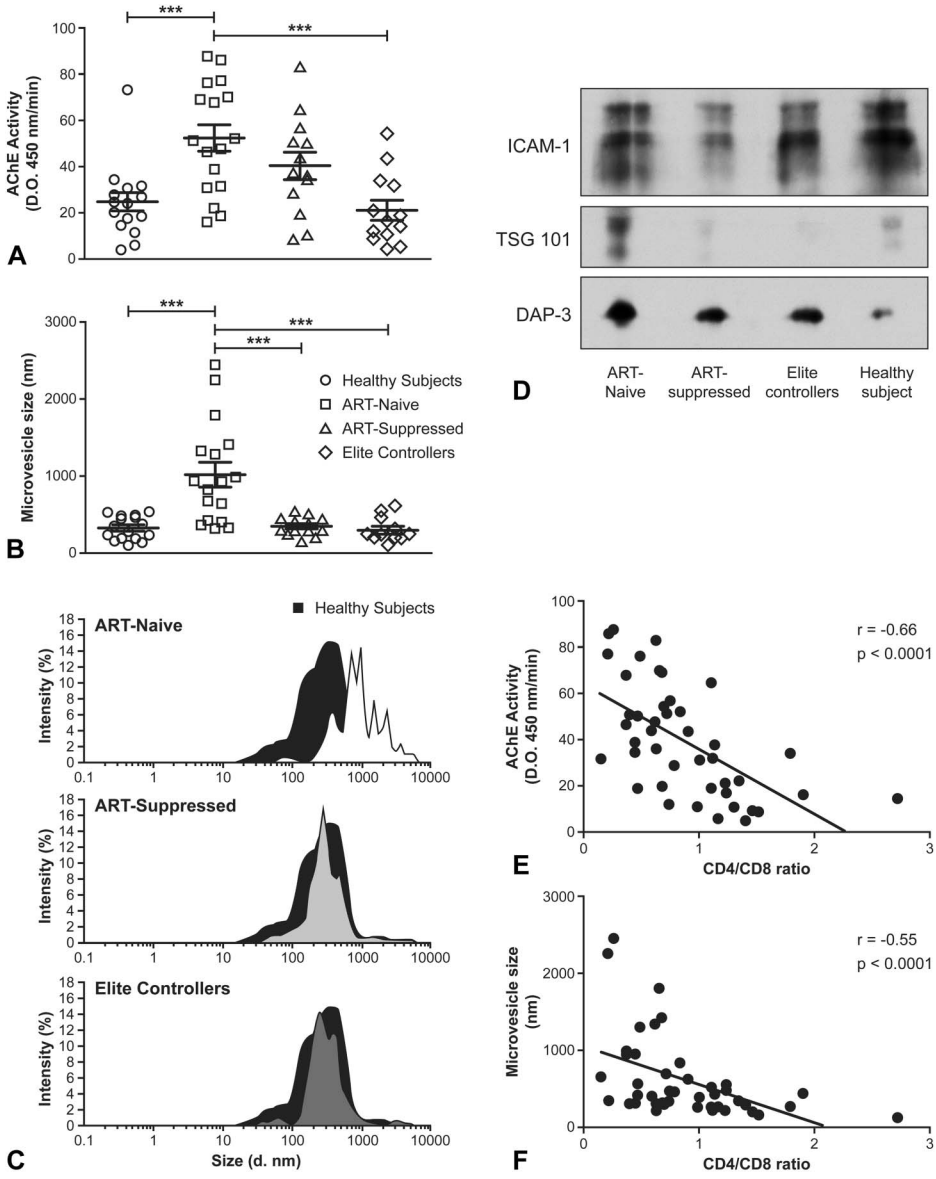

FIGURE 1. Characterization of EVs. Plasma was obtained from healthy individuals (n = 16) and HIV-1–infected individuals (n = 17 ART-naive, n = 13 ART-suppressed, n = 13 elite controllers). ExoQuick was used to precipitate EV fraction. A, AChE activity measured for each patient. B, DLS (Malvern Zeta nanosizer) sizing of EVs after fixation with 2% paraformaldehyde. C, Distribution of particle mean size, based on DLS (black indicates healthy individuals). D, Western blot of proteins precipitated from pooled plasma of each group. E and F, Correlations of AChE+ MV abundance and EV size with CD4/CD8 ratio in all HIV-infected patients, reported as Spearman r and P values (2-tailed). Asterisks denote statistically significant differences ($***P < 0.001$).

320 ± 37.5; ART-naive: 1017 ± 159.5; ART-suppressed: 343 ± 33.4; elite controllers: 298 ± 40.8; $P < 0.001$ for comparisons between ART-naive and healthy, ART-suppressed subjects, or elite controllers). To characterize EVs, we analyzed samples using Western blotting (Fig. 1D). TSG-101 is a protein involved in the biogenesis of multivesicular bodies and is considered as exosome marker.[14] It was found in larger amounts in plasma EVs from ART-naive HIV-1–infected patients. In contrast, ICAM-1–positive EVs are found in all plasma samples regardless of group. ICAM-1 is considered as a marker of plasma membranes. These data support the hypothesis that different EV populations are found in plasma depending on disease progression and that exosomes are more abundant in ART-naive patients. Finally, as we have found previously in exosomes derived from cells infected in vitro,[25] the mitochondrial ribosomal protein DAP-3, which might be involved in apoptosis, appeared to be more abundant in EVs obtained from pooled plasma of all HIV+ patient study groups, compared with healthy controls.

Exosome Abundance and EV Size Are Correlated With Markers of Disease Progression

To determine the potential of exosomes or EVs in general as biomarkers of HIV-1 pathogenesis, several correlations were examined. Tables 2 and 3 show the correlations of AChE activity and EV size with various clinical parameters, respectively, for the different categories of HIV-1 patients. There were correlations between vesicle-bound AChE activity and EV size and leukocyte counts in HIV-1 patients in general (last columns of both tables and bold values are significant values). Figure 1 shows how exosome levels (panel E) and EV size (panel F) correlate with CD4/CD8 ratio, which is considered to be an independent marker of disease progression,[36] as is the CD4 nadir.[37] Furthermore, our results indicate a significant correlation between CD4 nadir and exosome abundance in HIV-1–infected patients ($r = -0.3544$; $P < 0.04$). No correlation with patient age was observed, in contrast with the opposite correlation observed between exosome abundance and duration of HIV-1 infection in ART-suppressed ($r = 0.649$; $P < 0.02$) and elite controller patients ($r = -0.701$; $P < 0.02$).

MicroRNA Contained in Exosomes or EVs Purified From Plasma of HIV-1 Patients

Some studies have shown that infection or simple contact with HIV-1 may induce changes in T-cell microRNA profiles.[38] As the specific contents of EVs depend on the cells that secrete them, we hypothesized that EVs including exosomes from HIV-1 patients must contain microRNA. We therefore measured their miR-155, miR-223, and miR-92 (control) contents. Plasma samples were treated with proteinase K before ExoQuick purification to measure only intravesicular microRNA. This treatment eliminates large amount of microRNA potentially associated with high denisty Lipoprotein and low density Lipoprotein, proteins, or other EV-like surfaces.[39] Figure 2 shows that all 3 of these microRNAs are more abundant in EVs from ART-naive patients (6 of 8 patients for miR-155, 5 of 8 for miR-223, and all 8 for miR-92). AChE activity (panels D to F) was found correlated strongly with miR-155 ($r = -0.85$; $P = 0.007$) and miR-223 ($r = 0.87$; $P = 0.005$) contents, as was EV size (panels G to I). This was not the case for miR-92 (panel C) or miR-16 (data not shown). This microRNA enrichment was not likely due to an overall increase in total RNA incorporated into or associated with the extracellular components of EVs because proteinase K was used to eliminate such associations, as illustrated in panels J–M. Proteinase K treatment increased EV homogeneity, as shown by transmission electron microscopy (panels J and K) and DLS measurement (panels L and M). EVs from ART-naive patients contained less total RNA than did those from healthy or other HIV-1 patients (data not shown). Finally,

TABLE 2. Correlations Between Exosome Abundance (Based on AChE Assay) and Clinical Parameters

		HIV-1–Positive Subjects			
	Healthy Subjects (n = 16)	**ART-Naive (n = 17)**	**ART-Suppressed (n = 13)**	**Elite Controllers (n = 13)**	**HIV+ Subjects (n = 43)**
Viral load, $\log_{10}$ copies/mL	NA	r = 0.2500; $P = 0.3332$	NA	NA	NA
Years of infection	NA	r = −0.1068; $P = 0.6833$	**r = 0.6491; $P = 0.0164$**	**r = −0.7012; $P = 0.0268$**	**r = −0.4087; $P = 0.0088$**
CD4, cells/μL	r = −0.4456; $P = 0.0837$	**r = −0.5000; $P = 0.0410$**	r = −0.02201; $P = 0.9431$	r = 0.3956; $P = 0.1809$	**r = −0.3530; $P = 0.0202$**
CD8, cells/μL	**r = −0.5581; $P = 0.0247$**	r = 0.1961; $P = 0.4507$	r = 0.1703; $P = 0.5780$	r = 0.3411; $P = 0.2540$	**r = 0.4319; $P = 0.0038$**
CD4/CD8 ratio	r = 0.4071; $P = 0.1176$	r = −0.4758; $P = 0.0536$	r = −0.3274; $P = 0.2749$	r = −0.4176; $P = 0.1557$	**r = −0.6629; $P < 0.0001$**
Neutrophils, $\times 10^9$/L	r = −0.04176; $P = 0.8873$	**r = −0.5000; $P = 0.0410$**	r = −0.1293; $P = 0.6738$	r = −0.3664; $P = 0.2182$	**r = −0.5138; $P = 0.0004$**
Monocytes, $\times 10^9$/L	r = 0.4180; $P = 0.1369$	r = −0.00984; $P = 0.9701$	**r = −0.5824; $P = 0.0367$**	r = 0.03586; $P = 0.9074$	**r = −0.3634; $P = 0.0166$**
Platelets, $\times 10^9$/L	r = −0.1870; $P = 0.5220$	r = −0.2475; $P = 0.3381$	r = 0.07143; $P = 0.8166$	r = −0.2418; $P = 0.4262$	**r = −0.3783; $P = 0.0124$**
Age, yrs	r = 0.3058; $P = 0.2494$	r = 0.1698; $P = 0.5148$	r = 0.02213; $P = 0.9428$	r = −0.2929; $P = 0.3820$	r = −0.1679; $P = 0.2942$
CD4 nadir	NA	r = −0.4559; $P = 0.0759$	r = −0.2091; $P = 0.4930$	r = −0.8208; $P = 0.1333$	**r = −0.3544; $P = 0.0397$**

All correlations are reported as Spearman r and P values (2-tailed).
NA, not applicable.

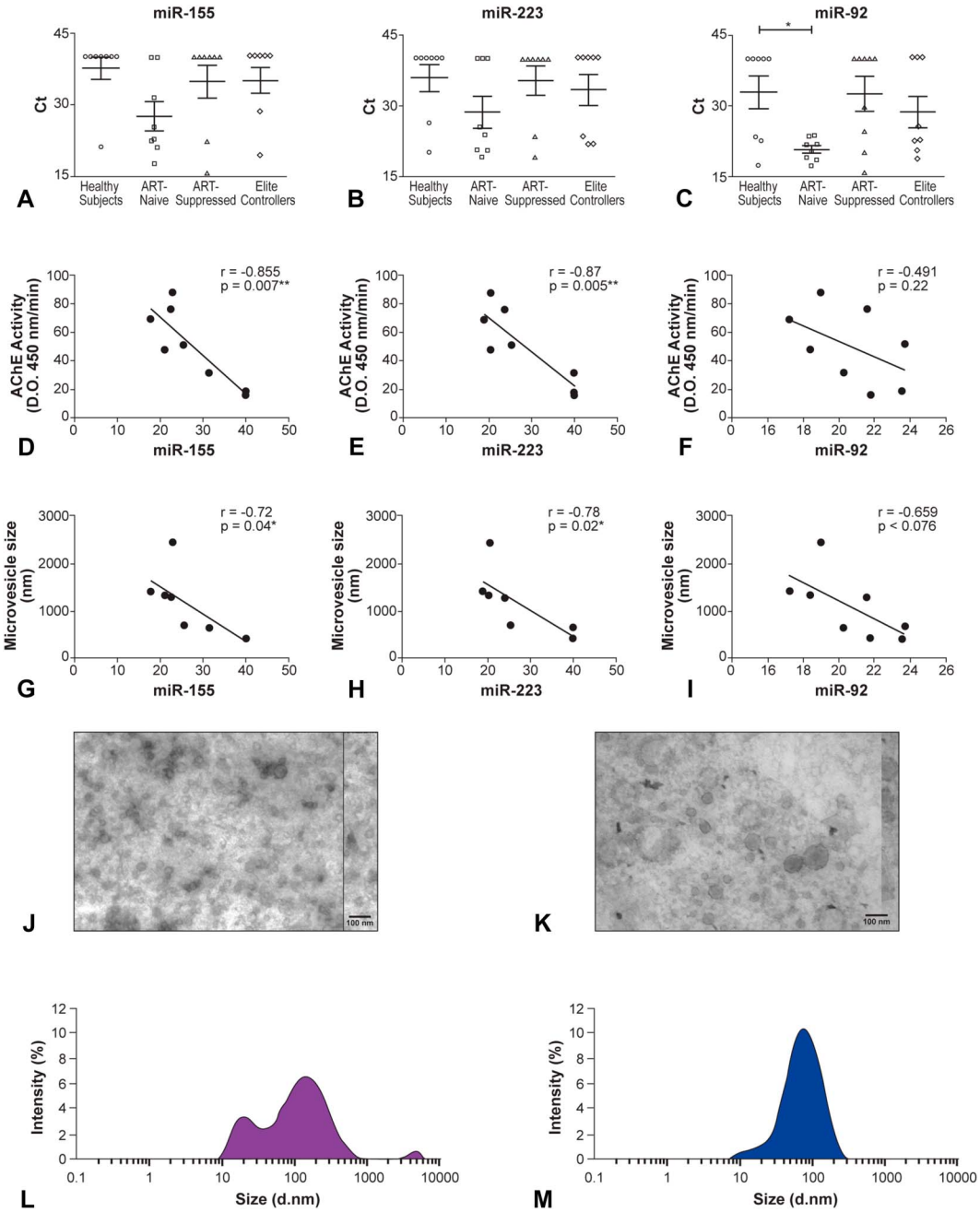

FIGURE 2. Detection of selected microRNAs in plasma EVs and correlation with AChE activity and size of EVs. Plasma obtained from healthy individuals (n = 8) and HIV-1–infected individuals (n = 8 ART-naive, n = 8 ART-suppressed, n = 8 elite controllers) was treated with proteinase K, and ExoQuick was used to precipitate EV fraction. MicroRNA miR-155 (A), mir-223 (B), and miR-92 (C) present in exosomes and MVs were amplified as described in the "Materials and Methods" section. Panels (D–F) show the correlation between microRNA relative abundance and AChE activity for ART-naive patients. Panels (G–I) show the correlation between microRNA abundance and EV size for ART-naive patients. All correlations are reported as Spearman r and *P* values (2-tailed). Asterisks denote statistically significant differences (*$P < 0.05$, **$P < 0.01$). Panels (J and K) show representative electron microscopy images of exosomes. Panels (L and M) show plasma MV size distribution, based on DLS measurement. Samples in (K and M) were treated with proteinase K.

these results nevertheless suggest possible enrichment in microRNA in ART-naive patients, although only miR-155 and miR-233 levels were correlated quantitatively with exosomes and EV size, in contrast with miR-92 and miR-16.

DISCUSSION

Exosome production is aptly described in the cancer literature as an intercellular communication strategy and exosomes themselves as diagnostic and prognostic markers.[22]

TABLE 3. Correlations Between EV Size Distribution and Clinical Parameters

		HIV-1–Positive Subjects			
	Healthy Subjects (n = 16)	**ART-Naive (n = 17)**	**ART-Suppressed (n = 13)**	**Elite Controllers (n = 13)**	**HIV+ Subjects (n = 43)**
Viral load, $\log_{10}$ copies/mL	NA	r = 0.0392; *P* = 0.8812	NA	NA	NA
Years of infection	NA	r = 0.0630; *P* = 0.8100	r = 0.4466; *P* = 0.1260	r = −0.09147; *P* = 0.8113	**r = −0.5438; *P* = 0.0003**
CD4, cells/μL	r = −0.1007; *P* = 0.7107	r = −0.2255; *P* = 0.3842	r = −0.3164; *P* = 0.2923	**r = 0.5970; *P* = 0.0312**	**r = −0.3579; *P* = 0.0184**
CD8, cells/μL	**r = −0.5389; *P* = 0.0313**	r = 0.3676; *P* = 0.1466	r = −0.2967; *P* = 0.3249	r = 0.5152; *P* = 0.0716	**r = 0.3131; *P* = 0.0409**
CD4/CD8 ratio	**r = 0.5211; *P* = 0.0385**	r = −0.3262; *P* = 0.2013	r = −0.04402; *P* = 0.8865	r = −0.4215; *P* = 0.1514	**r = −0.5554; *P* = 0.0001**
Neutrophils, $\times 10^9$/L	r = 0.4198; *P* = 0.1351	r = −0.2059; *P* = 0.4279	r = −0.1183; *P* = 0.7003	**r = −0.6359; *P* = 0.0195**	**r = −0.4722; *P* = 0.0014**
Monocytes, $\times 10^9$/L	**r = 0.5699; *P* = 0.0334**	r = 0.1341; *P* = 0.6079	r = −0.4615; *P* = 0.1124	r = −0.3370; *P* = 0.2601	r = −0.2263; *P* = 0.1444
Platelets, $\times 10^9$/L	r = −0.2200; *P* = 0.4498	r = −0.1887; *P* = 0.4682	r = 0.01099; *P* = 0.9716	**r = −0.6520; *P* = 0.0157**	**r = −0.5203; *P* = 0.0003**
Age, yrs	r = 0.2629; *P* = 0.3252	r = −0.0619; *P* = 0.8132	r = 0.2600; *P* = 0.3909	r = 0.5996; *P* = 0.0512	r = −0.2242; *P* = 0.1587
CD4 nadir	NA	r = 0.0630; *P* = 0.8100	r = 0.4466; *P* = 0.1260	r = −0.0606; *P* = 0.8679	r = −0.0348; *P* = 0.8449

All correlations are reported as Spearman r and *P* values (2-tailed).
NA, not applicable.

Information on exosomes in chronic viral infections including HIV infection remains limited. We have previously shown in vitro that DCs incubated with HIV-1 produce large amounts of exosomes containing proapoptotic molecules.[25] To study how EVs might reflect HIV-1 infection status in vivo, we analyzed plasma EVs from HIV-1 patients and evaluated the relationship between these particles and patient virological and immunological status. We thus observed increased abundance of exosomes and the exosome-associated protein called TSG-101 in ART-naive HIV-1–infected patients compared with elite controllers and uninfected control subjects. Previous studies have shown that both TSG-101 and AChE may be found in some exosome populations.[13,14,33] Our results show that exosomes are more abundant in the EV population of ART-naive patients than of other patient groups. In addition, EV hydrodynamic size was larger in ART-naive patients than in ART-treated subjects (ART-suppressed) or in elite controllers. Presenting with undetectable plasma viral load and having maintained nearly normal CD4 T-cell counts without receiving ART, elite controllers had exosome abundance and EV size comparable with those of control subjects. The differences in EV size and exosome abundance were associated with parameters reflecting disease progression. For example, size and abundance were associated negatively with CD4/CD8 ratio (recognized as an independent marker of disease progression) and hence with CD4 T-cell count, as well as with neutrophil and platelet counts, and positively with CD8 T-cell numbers. It is especially noteworthy that EV size and the presence of AChE were strongly correlated with the number of years of infection, independently of treatment status, patient age, and disease progression. However, only in elite controllers was a negative correlation observed between exosomes and duration of infection, possibly due to their high level of control over HIV replication. These findings provide novel information on the potential role of EVs and exosomes as biomarkers in HIV-1 disease progression and on the effect of ART.

The ratio of CD4/CD8 cells and more particularly CD4 T-cell nadir are predictors of immune activation level, both factors being associated with exosomes in HIV-1–infected patients, whether treated or untreated.[36,37] Immune activation–related apoptosis is considered to be a major mechanism of CD4 T-cell death. The increased abundance of exosomes may result in part from their ability to induce apoptosis of CD4 T cells, which Lenassi et al[26] have shown in vitro as we have, and from infection of naive CD4 T cells, as shown more recently.[27]

Other studies have shown that apoptotic vesicles are released from antigen-presenting cells and further induce T-cell and monocyte apoptosis.[9,31] It is known that apoptotic vesicles are larger than exosomes.[12] Their enhanced release during HIV-1 infection may explain the broad size distribution of EVs in the plasma of ART-naive patients. In addition, detection of mitochondrial protein DAP-3 (Fig. 1D) confirms our in vitro study showing its presence in exosomes derived from HIV-1–infected cells.[25] The presence of apoptotic effector protein DAP-3 in EVs from HIV+ patients suggests that this protein may contribute to the cell death observed during chronic HIV infection. However, this needs to be confirmed in further studies.

Depletion of CD4 T cells and increased number of CD8 T cells illustrate the disruption of the immune system caused by infection. The activation phenotype of CD4 and CD8 T cells is another hallmark of disease evolution. More recently, expression of CD38 and HLA-DR has been attributed to exosomes.[40] In addition, enrichment of exosomes from HIV-1 patients with several cytokines points toward an additional role for exosome contents in immune activation and disease progression.[40] Better understanding of the mechanisms associated with changes in CD4/CD8 ratio could be helpful in the control of disease progression.

Another possibility is that microRNA contained in EVs contributes to the changes that occur early during HIV-1 infection. Studies in mice show that miR-155 plays a role in the development of an effective antiviral effector CD8 response[41] and seems to be involved in increasing the

numbers of regulatory T cells.[42] Both cell types are known to increase during HIV-1 pathogenesis. The strong correlation between exosomes bearing both microRNAs involved in the regulation of immune response or inflammation and disease strongly suggests that analysis of plasma exosome abundance, EV size, and microRNA content could provide a unique and accurate fingerprint of local cellular activation and progression of inflammation and pathogenesis. We note with interest that the importance of miR-155 in the regulation of HIV-1 latency has been described recently.[43] Long-term monitoring of miR-155 in plasma EVs might provide valuable information on HIV-1 latency status. However, changes in microRNA content need to be followed in a longitudinal study in order to confirm this.

This study has shown for the first time that the presence of exosomes is correlated with duration of infection, CD4 nadir, and neutrophil cell counts and more importantly with 2 microRNAs (miR-155 and miR-223) involved in the regulation of immune and inflammatory responses. Overall, our findings will be helpful in future investigations of how the specific contents of plasma EVs participate in the immune deregulation that occurs after HIV-1 infection and already provide novel information on the role of EVs and exosomes as biomarkers in HIV-1 disease progression. Their clinical value as markers of response to treatment with antiapoptotic or other new therapeutic strategies in HIV-infected patients may also be considerable. EV analysis could serve as an excellent companion diagnostic. Over the longer term, modulation by pharmacological inhibitors or elimination by immune capture of EVs produced specifically in response to viral infection might contribute to reducing the deleterious effects of immune activation. These considerations require further study.

ACKNOWLEDGMENTS

The authors thank Dr. Stephen Davids for assistance in editing this manuscript and for constructive comments, Angie Massicotte for technical assistance, and Dr. Marc Pouliot and Ms. Cynthia Laflamme for access to quantitative polymerase chain reaction platform and technical assistance, respectively. They acknowledge the Bioimaging Platform of the Infectious Disease Research Center, funded by an equipment and infrastructure grant from the Canadian Foundation for Innovation (CFI), and Julie-Christine Levesque for microscopy analysis.

REFERENCES

1. Deeks SG, Tracy R, Douek DC. Systemic effects of inflammation on health during chronic HIV infection. *Immunity*. 2013;39:633–645.
2. Pereyra F, Lo J, Triant VA, et al. Increased coronary atherosclerosis and immune activation in HIV-1 elite controllers. *AIDS*. 2012;26:2409–2412.
3. Klatt NR, Chomont N, Douek DC, et al. Immune activation and HIV persistence: implications for curative approaches to HIV infection. *Immunol Rev*. 2013;254:326–342.
4. Brenchley JM, Schacker TW, Ruff LE, et al. CD4+ T cell depletion during all stages of HIV disease occurs predominantly in the gastrointestinal tract. *J Exp Med*. 2004;200:749–759.
5. Gougeon ML, Laurent-Crawford AG, Hovanessian AG, et al. Direct and indirect mechanisms mediating apoptosis during HIV infection: contribution to in vivo CD4 T cell depletion. *Semin Immunol*. 1993;5:187–194.
6. Haase AT. Population biology of HIV-1 infection: viral and CD4+ T cell demographics and dynamics in lymphatic tissues. *Annu Rev Immunol*. 1999;17:625–656.
7. Doitsh G, Cavrois M, Lassen KG, et al. Abortive HIV infection mediates CD4 T cell depletion and inflammation in human lymphoid tissue. *Cell*. 2010;143:789–801.
8. Doitsh G, Galloway NL, Geng X, et al. Cell death by pyroptosis drives CD4 T-cell depletion in HIV-1 infection. *Nature*. 2014;505:509–514.
9. Gasper-Smith N, Crossman DM, Whitesides JF, et al. Induction of plasma (TRAIL), TNFR-2, fas ligand, and plasma microparticles after human immunodeficiency virus type 1 (HIV-1) transmission: implications for HIV-1 vaccine design. *J Virol*. 2008;82:7700–7710.
10. Buzas EI, Gyorgy B, Nagy G, et al. Emerging role of extracellular vesicles in inflammatory diseases. *Nat Rev Rheumatol*. 2014;10:356–364.
11. Baur AS. HIV-Nef and AIDS pathogenesis: are we barking up the wrong tree? *Trends Microbiol*. 2011;19:435–440.
12. Gyorgy B, Szabo TG, Pasztoi M, et al. Membrane vesicles, current state-of-the-art: emerging role of extracellular vesicles. *Cell Mol Life Sci*. 2011;68:2667–2688.
13. Robbins PD, Morelli AE. Regulation of immune responses by extracellular vesicles. *Nat Rev Immunol*. 2014;14:195–208.
14. Thery C, Ostrowski M, Segura E. Membrane vesicles as conveyors of immune responses. *Nat Rev Immunol*. 2009;9:581–593.
15. Lagos-Quintana M, Rauhut R, Lendeckel W, et al. Identification of novel genes coding for small expressed RNAs. *Science*. 2001;294:853–858.
16. O'Connell RM, Chaudhuri AA, Rao DS, et al. MicroRNAs enriched in hematopoietic stem cells differentially regulate long-term hematopoietic output. *Proc Natl Acad Sci U S A*. 2010;107:14235–14240.
17. O'Connell RM, Rao DS, Chaudhuri AA, et al. Physiological and pathological roles for microRNAs in the immune system. *Nat Rev Immunol*. 2010;10:111–122.
18. Seddiki N, Brezar V, Ruffin N, et al. Role of miR-155 in the regulation of lymphocyte immune function and disease. *Immunology*. 2014;142:32–38.
19. Laffont B, Corduan A, Ple H, et al. Activated platelets can deliver mRNA regulatory Ago2*microRNA complexes to endothelial cells via microparticles. *Blood*. 2013;122:253–261.
20. Taibi F, Metzinger-Le Meuth V, Massy ZA, et al. miR-223: an inflammatory oncomiR enters the cardiovascular field. *Biochim Biophys Acta*. 2014;1842:1001–1009.
21. Li M, Guan X, Sun Y, et al. miR-92a family and their target genes in tumorigenesis and metastasis. *Exp Cell Res*. 2014;323:1–6.
22. Corrado C, Raimondo S, Chiesi A, et al. Exosomes as intercellular signaling organelles involved in health and disease: basic science and clinical applications. *Int J Mol Sci*. 2013;14:5338–5366.
23. Pegtel DM, Cosmopoulos K, Thorley-Lawson DA, et al. Functional delivery of viral miRNAs via exosomes. *Proc Natl Acad Sci U S A*. 2010;107:6328–6333.
24. Ramakrishnaiah V, Thumann C, Fofana I, et al. Exosome-mediated transmission of hepatitis C virus between human hepatoma Huh7.5 cells. *Proc Natl Acad Sci U S A*. 2013;110:13109–13113.
25. Subra C, Simard S, Mercier S, et al. Dendritic cells Pulsed with HIV-1 release exosomes that promote apoptosis in CD4+ T lymphocytes. *J Clin Cell Immunol*. 2011. (S7:001. doi:10.4172/2155–9899.S7).
26. Lenassi M, Cagney G, Liao M, et al. HIV Nef is secreted in exosomes and triggers apoptosis in bystander CD4+ T cells. *Traffic*. 2010;11:110–122.
27. Arenaccio C, Chiozzini C, Columba-Cabezas S, et al. Exosomes from Human Immunodeficiency virus type-1 (HIV-1)-infected cells license quiescent CD4+ T lymphocytes to replicate HIV-1 through a Nef- and ADAM17-dependent mechanism. *J Virol*. 2014;88:11529–11539.
28. Arenaccio C, Chiozzini C, Columba-Cabezas S, et al. Cell activation and HIV-1 replication in unstimulated CD4+ T lymphocytes ingesting exosomes from cells expressing defective HIV-1. *Retrovirology*. 2014;11:46.
29. Izquierdo-Useros N, Naranjo-Gomez M, Erkizia I, et al. HIV and mature dendritic cells: Trojan exosomes riding the Trojan horse? *PLoS Pathog*. 2010;6:e1000740.
30. Narayanan A, Iordanskiy S, Das R, et al. Exosomes derived from HIV-1-infected cells contain trans-activation response element RNA. *J Biol Chem*. 2013;288:20014–20033.
31. Frleta D, Ochoa CE, Kramer HB, et al. HIV-1 infection-induced apoptotic microparticles inhibit human DCs via CD44. *J Clin Invest*. 2012;122:4685–4697.

32. Kadiu I, Narayanasamy P, Dash PK, et al. Biochemical and biologic characterization of exosomes and microvesicles as facilitators of HIV-1 infection in macrophages. *J Immunol.* 2012;189:744–754.
33. Cantin R, Diou J, Belanger D, et al. Discrimination between exosomes and HIV-1: purification of both vesicles from cell-free supernatants. *J Immunol Methods.* 2008;338:21–30.
34. Columba Cabezas S, Federico M. Sequences within RNA coding for HIV-1 Gag p17 are efficiently targeted to exosomes. *Cell Microbiol.* 2013;15:412–429.
35. Gilbert C, Rollet-Labelle E, Caon AC, et al. Immunoblotting and sequential lysis protocols for the analysis of tyrosine phosphorylation-dependent signaling. *J Immunol Methods.* 2002;271:185–201.
36. Taylor JM, Fahey JL, Detels R, et al. CD4 percentage, CD4 number, and CD4:CD8 ratio in HIV infection: which to choose and how to use. *J Acquir Immune Defic Syndr.* 1989;2:114–124.
37. Boulassel MR, Chomont N, Pai NP, et al. CD4 T cell nadir independently predicts the magnitude of the HIV reservoir after prolonged suppressive antiretroviral therapy. *J Clin Virol.* 2012;53:29–32.
38. Bignami F, Pilotti E, Bertoncelli L, et al. Stable changes in CD4+ T lymphocyte miRNA expression after exposure to HIV-1. *Blood.* 2012; 119:6259–6267.
39. Vickers KC, Palmisano BT, Shoucri BM, et al. MicroRNAs are transported in plasma and delivered to recipient cells by high-density lipoproteins. *Nat Cell Biol.* 2011;13:423–433.
40. Konadu KA, Chu J, Huang MB, et al. Association of cytokines with exosomes in the plasma of HIV-1-Seropositive individuals. *J Infect Dis.* 2015;211:1712–1716.
41. Lind EF, Elford AR, Ohashi PS. Micro-RNA 155 is required for optimal CD8+ T cell responses to acute viral and intracellular bacterial challenges. *J Immunol.* 2013;190:1210–1216.
42. Kohlhaas S, Garden OA, Scudamore C, et al. Cutting edge: the Foxp3 target miR-155 contributes to the development of regulatory T cells. *J Immunol.* 2009;182:2578–2582.
43. Ruelas DS, Chan JK, Oh E, et al. MicroRNA-155 Reinforces HIV latency. *J Biol Chem.* 2015;290:13736–13748.